Ultracold scattering properties of the short-lived Rb isotopes

James P. Burke, Jr. and John L. Bohn
JILA and the Department of Physics, University of Colorado, Boulder, Colorado 80309-0440
(Received 21 September 1998)

We compute the scattering properties of rubidium atoms at ultracold temperatures, placing special emphasis on the radioactive isotopes ^{82}Rb, ^{83}Rb, ^{84}Rb, and ^{86}Rb. In combination with the more ''conventional'' isotope ^{87}Rb, these species yield a wide variety of scattering behavior, with consequences for creating mixtures of Fermi-Fermi, Fermi-Bose, and Bose-Bose gases. In each of these mixtures we find at least one case where the interspecies scattering lengths can be tuned using an external magnetic field. These results should greatly broaden the prospects for quantum degenerate gases in future experiments. [S1050-2947(99)06802-X]

PACS number(s): 34.50.−s, 32.80.Pj

I. INTRODUCTION

From the standpoint of ultracold collisions, every atom that can be trapped is unlike every other. To take an example, the alkali-metal atom ^{87}Rb is ''user-friendly,'' having a large positive scattering length [1] that facilitates its cooling by forced evaporation, as well as giving it a measurable mean-field energy when Bose-condensed. Take two neutrons away, however, and ^{85}Rb has instead a negative scattering length [1], which hinders both its evaporative cooling and the stability of its condensate. In between, ^{86}Rb is a fermion for which the Pauli exclusion principle prohibits *s*-wave interactions at all, at least for identical spin states.

The rich variety of ultracold gases grows when we consider mixtures of different species. For instance, again in ^{87}Rb, mixtures of the total spin states $|f,m\rangle=|2,1\rangle$ and $|1,-1\rangle$ have a positive *mutual* scattering length [2], making them nearly immiscible. The intricate dynamics of the resulting clouds has been strikingly observed [3]. Mixed condensate systems with three components have also been observed in sodium using novel optical traps [4]. A proposal exists for condensate mixtures with an attractive interspecies interaction [5], which have yet to be realized.

The aforementioned work has focused on the abundant and stable rubidium isotopes ^{85}Rb and ^{87}Rb. However, experimentalists are now becoming adept at cooling and trapping short-lived radioisotopes as well. Such efforts have included francium [6], sodium [7], and potassium [8], as well as ^{82}Rb [9]. These experiments offer the intriguing possibility of using these relatively short-lived species in studies of degenerate Bose and Fermi gases.

In this paper we present scattering properties for a number of rubidium isotopes, as a guide to interesting possible experiments in these gases and their mixtures. We will consider the isotopes of mass number $A=82$, 83, 84, 86, and 87, whose lifetimes are reasonably long (see Table I). Any alkali-metal atom with nuclear spin I possesses a total spin $\mathbf{f}=\mathbf{I}+\mathbf{1/2}$, giving a total spin quantum number $f=I\pm1/2$. Thus Table I represents a total of 58 distinct spin states $|f,m\rangle_A$. Of these, only 26 are weak-field seeking states that can be trapped magnetically. Thus we can contemplate 26 different quantum degenerate gases, or 325 binary mixtures of these gases.

Rather than tax the reader's patience (and certainly our own), we will focus only on intra-isotope collisions, with the exception of collisions of various isotopes with ^{87}Rb (see below). We pare down the resulting list of candidates according to the following criteria: (i) collision partners must be immune to spin-exchange loss processes, owing to either symmetry or energy considerations; (ii) atoms must be viable candidates for evaporative cooling, having large elastic cross sections ($\sim10^{-11}$ cm^2); and (iii) atoms must have scattering properties which would provide potentially interesting consequences for degenerate gas studies. This last criterion includes the possibility of tuning interatomic interactions using a bias magnetic field [10]. This capability has in fact been recently realized experimentally [11,12] in other species.

II. MODEL

Construction of the Hamiltonian for the process $|f,m\rangle_A+|f',m'\rangle_{A'}$ begins with Born-Oppenheimer molecular potentials for the singlet and triplet electronic states of two Rb atoms. For this purpose we use Amiot's spectroscopically determined singlet potential [13] and Krause and Stevens' *ab initio* triplet potential [14]. We match these potentials smoothly onto a long range dispersion potential using coefficients (C_8,C_{10}) given in Ref. [15] and a long range spin exchange contribution [16]. We then transform these potentials into the separated-atom basis $|f,m\rangle_A|f',m'\rangle_{A'}$, and incorporate the hyperfine energies of these states, to construct a full Hamiltonian. In this basis the magnetic field Hamiltonian is also easily implemented. We perform scattering calcula-

TABLE I. Nuclear spin I, ground-state atomic hyperfine splittings Δ, and half-life τ of the Rb isotopes. A negative value of Δ indicates an ''inverted'' hyperfine structure. The half-life units are *m*, minutes; *d*, days; *y*, years.

Isotope	I	Δ (GHz)	τ
82	1	1.5474	1.273 *m*
83	5/2	6.3702	86.2 *d*
84	2	−3.08316	32.9 *d*
85	5/2	3.03573	stable
86	2	−3.94688	18.63 *d*
87	3/2	6.83468	$4.88(10^{10})y$

tions using a finite-element R-matrix procedure [17] in conjunction with the multichannel quantum-defect methods developed in Ref. [18].

One essential aspect of constructing our Hamiltonian is fine-tuning it to agree with all available experimental information on ultracold rubidium collisions. To allow this kind of flexibility we added corrections to the inner walls of the singlet and triplet potentials, effectively giving us control over their phase shifts [19]. This fine-tuning enabled us to match quantitatively the line shape of the recently measured magnetic-field-induced Feshbach resonance in ^{85}Rb collisions, which is perhaps the most sensitive measurement yet of ultracold scattering properties [12]. In addition, including a previously observed g-wave shape resonance [20] in ^{85}Rb allowed us to bound the value of the C_6 dispersion coefficient to 4700 ± 50 a.u. [12]. This value for C_6 is slightly larger but with smaller uncertainty than the value determined in Ref. [20] (4550 ± 100 a.u.).

Transplanting these potentials to other Rb isotopes can be justified by comparing our calculated ^{87}Rb scattering observables with the measured values. We find our calculated thermal averaged inelastic spin exchange rates [21], scattering length ratios [22], and d-wave shape resonance [1] all agree within the stated 1σ experimental uncertainties. In addition, we find 10 of the 12 measured d-wave ^{85}Rb bound states [23] within the 2σ error bars. The largest source of uncertainty for the other isotopes comes from the ±1 uncertainty in the number of bound states in the triplet potential [23]. These agreements give us confidence in the reliability of our predictions for all the other isotopes of rubidium. We present in Table II the singlet and triplet scattering lengths for various combinations of rubidium isotopes. The data in this table can also be used to evaluate the uncertainty in the scattering lengths, expressed in a compact form using a quantum-defect parametrization [18].

TABLE II. Singlet and triplet scattering lengths a (in a.u.) and quantum defects $\bar{\mu}$ (dimensionless) for the different Rb isotopic pairs given a constant $C_6=4700$ a.u. and $C_8=550\,600$ a.u. The uncertainty in the singlet quantum defect $\bar{\mu}_S$ is 0.0014 in all cases. Variations of the scattering lengths with C_6 and C_8 can be determined by the following formulas (see Refs. [12,18] for details): $\mu=\bar{\mu}+b_6(C_6-4700)-b_8(C_8-550\,600)$ and $a=-C^2\tan(\pi\mu)/[1+\mathcal{G}(0)\tan(\pi\mu)]$, where $C^2=0.957\,217(2mC_6)^{1/4}$, m is the reduced mass of the atom-pair, and $\mathcal{G}(0)=-1.0026$. The constant b_6 equals $7.5(10^{-5})$ for the singlet and $1.4(10^{-4})$ for the triplet. The constant b_8 is the same for both potentials and is given by $2.0(10^{-8})$. Information on both ^{85}Rb and ^{87}Rb is provided for completeness.

Pair	a_S	$\bar{\mu}_S$	a_T	$\bar{\mu}_T$
82-82	-38 ± 1	0.0612	$+151\pm10$	-0.491 ± 0.019
83-83	$+66\pm1$	-0.2021	$+81\pm3$	-0.262 ± 0.013
84-84	$+142\pm1$	-0.4678	$+15\pm3$	-0.033 ± 0.007
85-85	$+2400^{+600}_{-350}$	0.2603	-369 ± 16	0.194 ± 0.001
86-86	$+7\pm1$	-0.0144	$+211\pm7$	0.421 ± 0.007
87-87	$+90\pm1$	-0.2939	$+106\pm4$	-0.354 ± 0.003
82-87	$+55\pm1$	-0.1568	-40 ± 4	0.064 ± 0.004
83-87	-990^{+60}_{-70}	0.2263	-295 ± 7	0.184 ± 0.001
84-87	$+117\pm1$	-0.3952	$+550^{+45}_{-35}$	0.302 ± 0.004
85-87	$+11\pm1$	-0.0233	$+213\pm7$	0.418 ± 0.007
86-87	$+336\pm4$	0.3443	$+143\pm4$	-0.467 ± 0.010

III. FERMIONIC ISOTOPES

We consider first the fermionic isotopes, i.e., those with even values of A. The Pauli exclusion principle prohibits s-wave collisions of two identical fermions. Appreciable collision rates at sub-milliKelvin temperatures would therefore hinge on near-threshold p-wave shape resonances, which are absent in the rubidium isotopes, as our calculations show [24]. Consequently, evaporative cooling of these gases requires either a mixture of isotopes or a mixture of spin states. One possibility for sympathetically cooling fermions is to immerse them in a bath of bosonic atoms. Because evaporatively cooling ^{85}Rb itself is notoriously difficult [12], we will consider only ^{87}Rb for the mixed isotope cases.

Sympathetic cooling of ^{82}Rb by ^{87}Rb seems a difficult prospect at best. The only two possibilities for collisions between these two atoms that are immune to spin exchange are $|3/2,3/2\rangle_{82}+|2,2\rangle_{87}$ and $|1/2,-1/2\rangle_{82}+|1,-1\rangle_{87}$. Both of these combinations possess *negative* s-wave scattering lengths, primarily driven by the negative triplet scattering length $a_t(82-87)$ (Table II). Under these circumstances, the s-wave elastic partial cross section suffers a zero at low collision energies [see Fig. 1(a)]. An explanation for this effect, based on Levinson's theorem [25], has been given elsewhere [19]. For our purposes, the main point is that the first zero in the s-wave partial cross section will occur at the lowest energy for a small negative scattering length. As the magnitude of the negative scattering length is increased, the position of the first zero *increases* in energy. Typically, the first zero for a positive scattering length occurs at an energy large enough that higher partial waves will contribute considerably to the total cross section. The experimental consequences of this effect have been observed in ^{85}Rb [12]. However, we do find a magnetic-field-induced Feshbach resonance in the $|1/2,-1/2\rangle_{82}+|1,-1\rangle_{87}$ collision [see Fig. 1(b)]. The resonance could therefore be used to alter the energy dependence of the elastic cross section as demonstrated in Ref. [12]. By contrast, ^{84}Rb and ^{86}Rb are ideal candidates for sympathetic cooling with ^{87}Rb, having large positive triplet scattering lengths.

In addition, both ^{84}Rb and ^{86}Rb have an ''inverted'' hyperfine structure (see Table I), making $f=5/2$ the lower energy state in each case. In particular, this means that the process $|5/2,5/2\rangle_A+|5/2,3/2\rangle_A\rightarrow|5/2,5/2\rangle_A+|3/2,3/2\rangle_A$ is energetically forbidden at ultracold temperatures. Evaporatively cooling $|5/2,5/2\rangle_A$ and $|5/2,3/2\rangle_A$ states together might then be viable. Interestingly, however, in both cases the re-

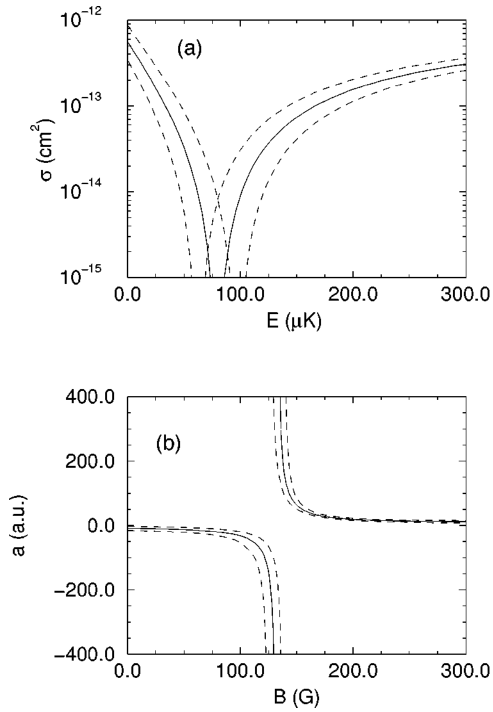

FIG. 1. (a) Elastic *s*-wave partial cross sections versus collision energy for $|3/2,3/2\rangle_{82}+|2,2\rangle_{87}$. The energy position of the first zero in the partial cross section is $E=80\pm 20\ \mu$K. (b) Scattering length versus magnetic field for the collision $|1/2,-1/2\rangle_{82}+|1,-1\rangle_{87}$. The zero energy resonance occurs at $B_0=132\pm 6$ G with a width of $\Delta=2\pm 1$ G. In both graphs the solid line represents the nominal value and dashed lines represent uncertainties.

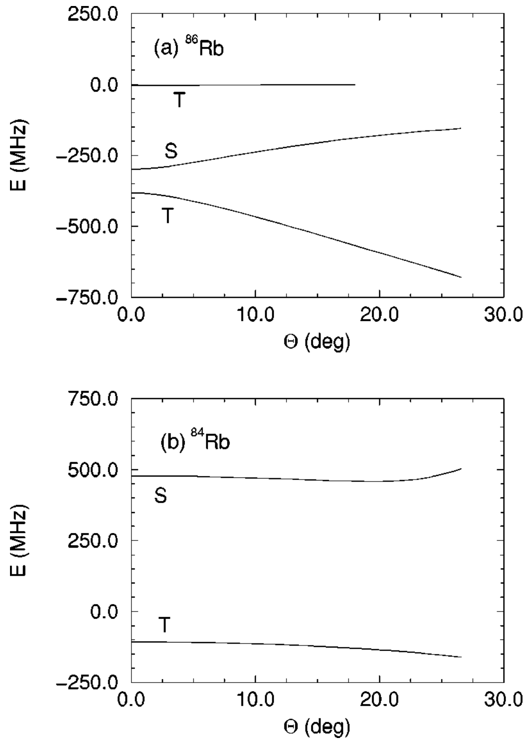

FIG. 2. Bound and pseudobound state positions versus the coupling parameter θ. The physical coupling strength is given by $\theta=26.57°$. The labels S and T refer to singlet or triplet states in the $\theta=0$ limit. Zero energy defines the entrance channel threshold. (a) $|5/2,5/2\rangle_{86}+|5/2,3/2\rangle_{86}$; (b) $|5/2,5/2\rangle_{84}+|5/2,3/2\rangle_{84}$.

sulting scattering length is *negative*, in spite of *positive* singlet and triplet scattering lengths (Table II). Such a result, contrary to the degenerate internal states (DIS) model of hyperfine state scattering [26], bears exploring here.

Neglecting magnetic dipole coupled channels, this is a coupled two-channel problem with the $|5/2,5/2\rangle_A+|3/2,3/2\rangle_A$ channel energetically closed as $R\to\infty$. The unitary frame transformation connecting the short range basis of total electronic S and nuclear I spin with the asymptotic hyperfine basis predicts that the entrance channel has 80% triplet character. The DIS model, which neglects hyperfine energies, would then predict ($a=0.8a_T+0.2a_S$), i.e., that both scattering lengths are reasonably large and positive.

In fact, the positions of bound states relative to the appropriate hyperfine thresholds are crucial for determining the actual scattering length. Let us explore this notion by describing the coupling in our two-channel system in terms of a mixing angle θ. We can model the potential as

$$\underline{V}=\underline{U}(\theta)\underline{V}^S\underline{U}^{\mathrm{T}}(\theta)+\underline{E}, \tag{1}$$

where $\underline{U}(\theta)$ is a standard 2×2 orthogonal rotation matrix, $\underline{V}^S$ is a diagonal matrix of singlet and triplet Born-Oppenheimer potentials, and $\underline{E}$ is a diagonal matrix of hyperfine energies. The model in the uncoupled limit ($\theta=0$) is simply a triplet potential connected to the lowest hyperfine threshold and a singlet channel with one additional unit of hyperfine energy.

Figure 2 shows the evolution of the bound state energies as θ grows from zero to its physical value, $\theta=26.57°$. In ^{86}Rb [Fig. 2(a)], we find an extremely high-lying bound state in the uncoupled limit ($\theta=0$) which accounts for the large triplet scattering length. As the coupling is turned on, a nearly degenerate pair of bound states, one singlet and one triplet, begins to repel each other. Eventually the singlet state ''pushes'' the high-lying triplet state above threshold, resulting in a negative scattering length. In ^{84}Rb [Fig. 2(b)] the highest-lying bound state is rather deep for $\theta=0$, in accord with this isotope's small positive triplet scattering length. As the coupling is turned on, this bound state interacts with a ''singlet'' state lying above threshold pushing it still deeper into the potential, ultimately producing a negative scattering length. In both cases, the positions of the singlet states *relative to the upper hyperfine threshold* are the determining factors in the physical scattering length.

This interesting result implies a net attraction between $|5/2,5/2\rangle_A$ and $|5/2,3/2\rangle_A$ spin states, which could have important consequences for forming Cooper pairs in these fermionic systems [27]. On the other hand, the negative scattering lengths in these species again produce zeros in their *s*-wave cross sections, as shown in Fig. 3. The good news is that ^{84}Rb exhibits a Feshbach resonance in the presence of modest-sized magnetic fields [Fig. 4(a)]. This resonance could then be used to move the position of the *s*-wave partial cross-section zero to higher collision energies [Fig. 4(b)], allowing the atoms to be evaporatively cooled into the degenerate regime. The extremely large width of this resonance eliminates the need for accurate control of magnetic field strengths. The resonance would also allow the experimental-

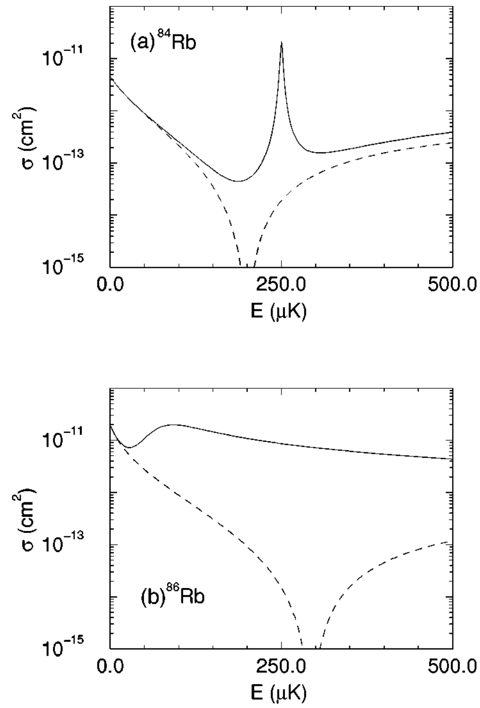

FIG. 3. Elastic cross sections versus collision energy using our nominal potentials. Solid lines represent the total cross section, dashed lines indicate the *s*-wave contribution. The energy position of the first zero in the *s*-wave partial cross section is 200 ± 30 μK for (a) and 295$\pm$25 μK for case (b). (a) $|5/2,5/2\rangle_{84}+|5/2,3/2\rangle_{84}$. The feature near 250 μK in the total cross section is an *f*-wave shape resonance. Although we find the position of this resonance is uncertain to ± 150 μK, it does not contribute over a broad enough energy range to compensate for the zero in the *s*-wave cross section. (b) $|5/2,5/2\rangle_{86}+|5/2,3/2\rangle_{86}$. We find a broad pseudo-*p*-wave shape resonance near 60 μK. The height of the *p*-wave centrifugal barrier is roughly 80 μK. In this case, the strong *p*-wave scattering is probably enough to compensate for the zero in the *s*-wave cross section.

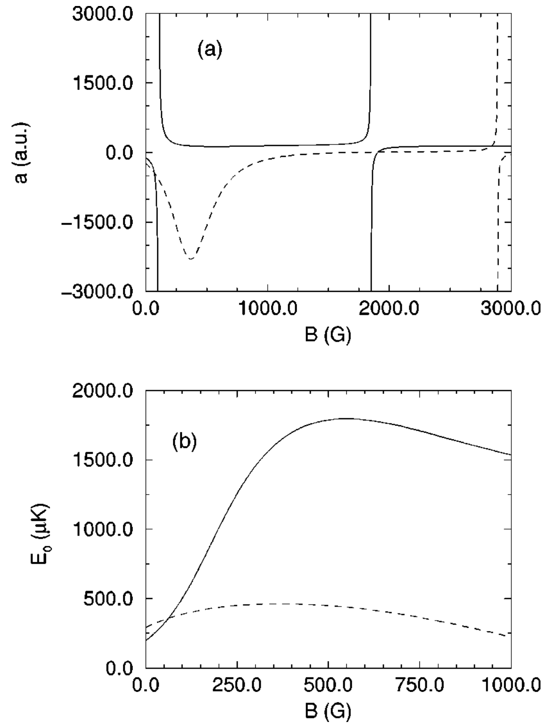

FIG. 4. Solid lines represent $|5/2,5/2\rangle_{84}+|5/2,3/2\rangle_{84}$ collision, dashed lines represent the same spin state collision for ^{86}Rb. (a) Scattering lengths versus applied magnetic field. The zero energy position of the low-field ^{84}Rb resonance is 106$\pm$9 G. (b) Energy position E_0 of the first *s*-wave partial cross-section zero versus applied magnetic field.

ist a means to study both repulsive and attractive effective interaction between atoms in a single system.

We find that in the ^{86}Rb case, a magnetic field will also influence the scattering length, but will change its sign only at very large fields $\approx$2800 G [Fig. 4(a)]. The position of the cross-section zero can be moved to a higher collision energy (Fig. 4b), but to a lesser extent than in ^{84}Rb. However, in this case the *s*-wave zero is not a major problem since the enhanced *p*-wave scattering [24] should enable the experimentalist to evaporatively cool the ^{86}Rb mixed spin states without a magnetic field bias. Of course, introducing a bias field of a few hundred gauss would increase the low energy [$\sim$50 μK, see Fig. 3(b)] total cross section by roughly a factor of 3.

In both cases the variation of scattering length with magnetic field is somewhat unusual, and so we dwell on this aspect for a moment. Figure 5 reports the variation of the two thresholds with magnetic field (solid lines), along with the variation of the positions of high-lying bound states (dashed lines). In both cases we observe a network of avoided crossings that push bound states closer to, or farther from, the incident (lower) threshold. For example, in ^{84}Rb [Fig. 5(a)], a bound state that has singlet character in the $\theta=0$ limit plummets just barely below threshold at $\approx$100 G, accounting for the initial resonance in the ^{84}Rb scattering length, which goes first negative, then recovers to a positive value. This same bound state hovers near threshold until about 1850 G of field strength, at which point a lower-lying, predominantly triplet bound state ''pushes'' it back above threshold. (This event is labeled ''*r*'' in the figure.) The result is then a resonant scattering length that first rises to $+\infty$, then reappears with negative values.

In the case of ^{86}Rb [Fig. 5(b)], a triplet bound state lying below the incident threshold first drops relative to this threshold, then rises again, owing to its avoided crossing with a singlet level above threshold. The scattering length thus tends toward more negative values, but recovers before going positive. In addition, we note that this resonance has an unusually large magnetic-field width, of several hundred gauss. The origin of this width is an extremely strong coupling between the incident and resonant channels. One measure of the strength of this coupling is the value of the ''short-range'' scattering matrix [18,28], whose absolute square is plotted versus B in Fig. 6. The matrix element S_{12}^{sr} represents the probability amplitude for flux incident in the $|5/2,5/2\rangle+|5/2,3/2\rangle$ channel to scatter back into the $|5/2,5/2\rangle+|3/2,3/2\rangle$ channel. Figure 6 puts this probability at nearly unity, indicating an extremely large coupling.

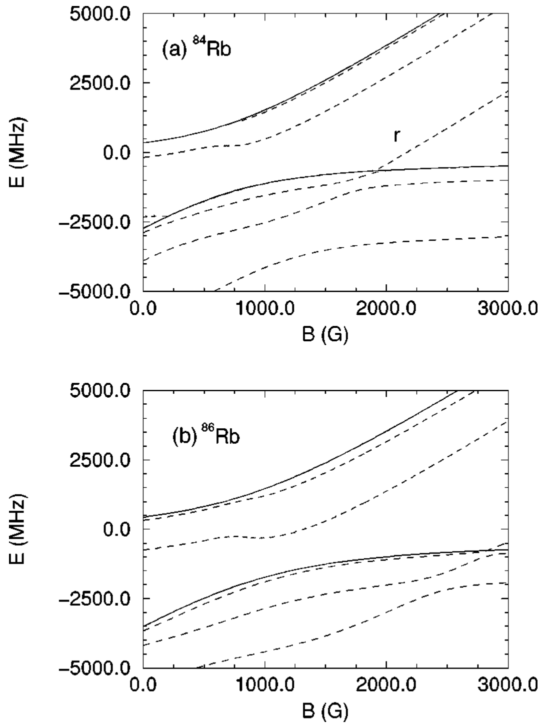

FIG. 5. Bound and pseudobound state positions versus magnetic field. Solid lines represent thresholds, dashed lines represent the bound and pseudobound state positions. (a) $|5/2,5/2\rangle_{84}+|5/2,3/2\rangle_{84}$. The state described in the text is labeled *r*. Its position when below threshold is not visible on this scale. (b) $|5/2,5/2\rangle_{86}+|5/2,3/2\rangle_{86}$.

IV. BOSONIC ISOTOPES

We have already dealt at length with mixtures of the bosonic rubidium isotopes ^{85}Rb and ^{87}Rb [5], and so here we will focus on ^{83}Rb. It exhibits scattering properties remarkably similar to those of ^{87}Rb. Namely, its singlet and triplet scattering lengths (see Table II) are relatively large, positive, and very nearly the same. By itself, then ^{83}Rb adds little to the field of BEC. However, mixtures of ^{83}Rb with

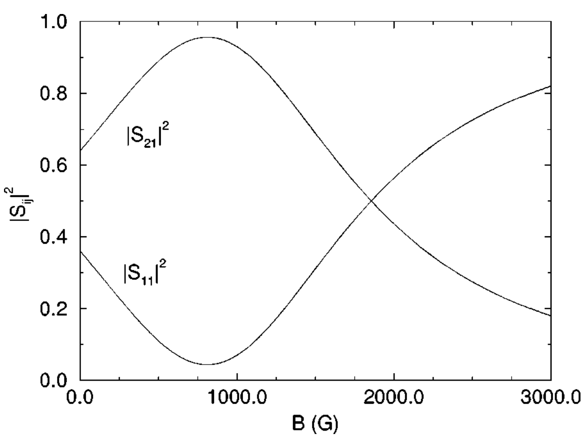

FIG. 6. Short-range scattering probabilities $|S^{sr}_{ij}|^2$ versus magnetic field for a $|5/2,5/2\rangle_{86}+|5/2,3/2\rangle_{86}$ collision. S^{sr} is derived in the standard way from a short-range *K* matrix [18] calculated at an internuclear distance of 35 a.u.

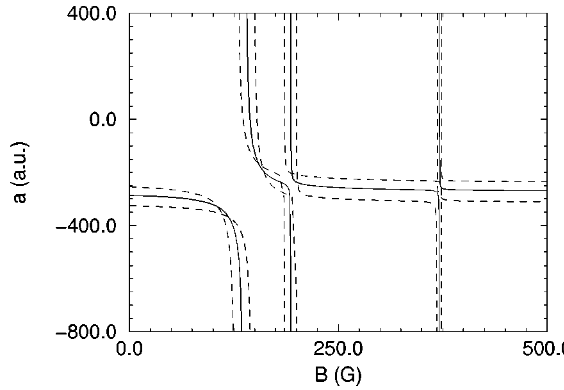

FIG. 7. Scattering length versus applied magnetic field for a collision of $|2,-2\rangle_{83}+|1,-1\rangle_{87}$ atoms. Solid lines represent the nominal value, dashed lines represent uncertainties. The zero energy positions of the resonance peaks are 138 ± 10 G, 193 ± 8 G, and 371 ± 3 G. The low-field resonance has a width of $\Delta=6.5\pm2.5$ G. The two higher field resonances are extremely narrow $\ll1$ G.

^{87}Rb open up some exciting possibilities for double condensates.

We first note that collisions between the spin ''stretched'' states $|3,3\rangle_{83}$ and $|2,2\rangle_{87}$ have a large negative scattering length (see Table II), which is not surprising since the ^{83}Rb-^{87}Rb reduced mass is very nearly the same as the reduced mass of two ^{85}Rb atoms. Within the Thomas-Fermi approximation, double condensates with scattering lengths a_1 and a_2 are unstable whenever their mutual scattering length a_{12} satisfies $|a_{12}|>\sqrt{a_1a_2}$ [29,30]. This relationship holds strictly only for isotropic like-species condensates. However, a more general derivation [31] for anisotropic mixed-isotope double condensates shows the instability remains. The nature of this stability has yet to be fully interpreted, particularly in the case of a_{12} negative. The 83-87 mixture would provide one means of probing this phenomenon.

Finally, we consider these isotopes in their lower hyperfine manifolds, i.e., collisions between $|2,-2\rangle_{83}$ and $|1,-1\rangle_{87}$. The scattering length between these partners is again negative, but in this case there exists an accessible Feshbach resonance (Fig. 7). Thus, unlike the ^{85}Rb-^{87}Rb case considered in Ref. [5], in this system we can envision two large condensates (each having $a>0$) with a tunable interspecies interaction. This capability will enable detailed studies of double condensates all the way from completely overlapping to utterly immiscible [32,33], in particular at the stability limits where $|a_{12}|\approx\sqrt{a_1a_2}$.

V. SUMMARY

In conclusion, we have shown that the short-lived Rb isotopes provide collisional properties which could enhance the study of degenerate Bose and Fermi gases. We predict a Feshbach resonance in the collisions of two ^{84}Rb atoms which could in principle allow the experimentalist to investigate both magnetic domain formation and Cooper pairing within a single atomic species. We find a Feshbach resonance in the ^{83}Rb-^{87}Rb mixed-isotope collision which should in principle allow the experimentalist to investigate the collapse of a double Bose condensate. In addition, we find that sympathetically cooling ^{84}Rb or ^{86}Rb with ^{87}Rb should also be feasible.

ACKNOWLEDGMENTS

We would like to thank Xinxin Zhao and T. L. Ho for expressing an interest in this project and Chris Greene for many useful comments and suggestions. This work has been supported by the National Science Foundation.

[1] H. M. J. M. Boesten, C. C. Tsai, J. R. Gardner, D. J. Heinzen, and B. J. Verhaar, Phys. Rev. A **55**, 636 (1997).

[2] J. P. Burke, Jr., J. L. Bohn, B. D. Esry, and C. H. Creene, Phys. Rev. A **55**, R2511 (1997).

[3] D. Hall, M. R. Matthews, J. R. Ensher, C. E. Wieman, and E. A. Cornell, Phys. Rev. Lett. **81**, 1539 (1998).

[4] D. M. Stampur-Kurn, M. R. Andrews, A. P. Chikkatur, S. Inouye, H. J. Miesner, J. Stenger, and W. Ketterle, Phys. Rev. Lett. **80**, 2027 (1998).

[5] J. P. Burke, Jr., J. L. Bohn, B. D. Esry, and C. H. Greene, Phys. Rev. Lett. **80**, 2097 (1998).

[6] Z.-T. Lu, K. L. Corwin, K. R. Vogel, C. E. Wieman, T. P. Dinneen, J. Maddi, and H. Gould, Phys. Rev. Lett. **79**, 994 (1997); J. E. Simsarian, L. A. Orozco, G. D. Sprouse, and W. Z. Zhao, Phys. Rev. A **57**, 2448 (1998).

[7] Z.-T. Lu, C. J. Bowers, S. J. Freedman, B. K. Fujikawa, J. L. Mortara, S-Q. Shang, K. P. Coulter, and L. Young, Phys. Rev. Lett. **72**, 3791 (1994).

[8] J. A. Behr *et al.*, *Program and Abstracts of Contributed Papers for the XVI ICAP Meeting*, edited by W. E. Baylis and G.W.F. Drake (University of Windsor, Windsor, Ontario, 1998), p. 62.

[9] R. Guckert, X. Zhao, S. G. Crane, A. Hime, W. A. Taylor, D. Tupa, D. J. Vieira, and H. Wollnik, Phys. Rev. A **58**, R1637 (1998).

[10] E. Tiesinga, B. J. Verhaar, and H. T. C. Stoof, Phys. Rev. A **47**, 4114 (1993).

[11] S. Inouye, M. R. Andrews, J. Stenger, H. J. Miesner, D. M. Stamper-Kurn, and W. Ketterle, Nature (London) **392**, 151 (1998); Ph. Couteille, R. S. Freeland, D. J. Heinzen, F. A. van Abeelen, and B. J. Verhaar, Phys. Rev. Lett. **81**, 69 (1998).

[12] J. L. Roberts, N. R. Claussen, J. P. Burke, Jr., C. H. Greene, E. A. Cornell, and C. E. Wieman, Phys. Rev. Lett. **81**, 5109 (1998).

[13] C. Amiot, J. Chem. Phys. **93**, 8591 (1990).

[14] M. Krausse and W. J. Stevens, J. Chem. Phys. **93**, 4236 (1990).

[15] M. Marinescu, H. R. Sadeghpour, and A. Dalgarno, Phys. Rev. A **49**, 982 (1994).

[16] B. M. Smirnov and M. I. Chibisov, Zh. Éksp. Teor. Fiz. **48**, 939 (1965) [Sov. Phys. JETP **21**, 624 (1965)].

[17] J. P. Burke, Jr., C. H. Greene, and B. D. Esry, Phys. Rev. A **54**, 3225 (1996).

[18] J. P. Burke, Jr., C. H. Greene, and J. L. Bohn, Phys. Rev. Lett. **81**, 3355 (1998).

[19] J. L. Bohn, J. P. Burke, Jr., C. H. Greene, H. Wang, P. L. Gould, and W. C. Stwalley (submitted).

[20] H. M. J. M. Boesten, C. C. Tsai, B. J. Verhaar, and D. J. Heinzen, Phys. Rev. Lett. **77**, 5194 (1996).

[21] C. J. Myatt, E. A. Burt, R. W. Ghrist, E. A. Cornell, and C. E. Wieman, Phys. Rev. Lett. **78**, 586 (1997).

[22] M. R. Matthews, D. S. Hall, D. S. Jin, J. R. Ensher, C. E. Wieman, E. A. Cornell, F. Dalfovo, C. Minniti, and S. Stringari, Phys. Rev. Lett. **81**, 243 (1998).

[23] C. C. Tsai, R. S. Freeland, J. M. Vogels, H. M. J. M. Boesten, B. J. Verhaar, and D. J. Heinzen, Phys. Rev. Lett. **79**, 1245 (1997).

[24] We do find a broad pseudoshape resonance at $E \simeq 60\ \mu$K in a p-wave collision of two ^{86}Rb atoms. Evaporatively cooling pure spin states of ^{86}Rb could therefore be possible down into the tens of μK. However, sub-μK cooling would still require other approaches.

[25] N. F. Mott and H. S. W. Massey, *Atomic Collisions* (Oxford University Press, New York, 1965), p. 156.

[26] A. Dalgarno and M. R. H. Rudge, Proc. R. Soc. London, Ser. A **286**, 519 (1965); H. T. C. Stoof, J.M.V.A. Koelman, and B. J. Verhaar, Phys. Rev. B **38**, 4688 (1988).

[27] H. T. C. Stoof, Phys. Rev. Lett. **76**, 10 (1996); A. G. K. Modowi and A. J. Leggett, J. Low Temp. Phys. **104**, 625 (1997).

[28] M. Aymar, C. H. Greene, and E. Luc-Koenig, Rev. Mod. Phys. **68**, 1015 (1996).

[29] T. L. Ho and V. B. Shenoy, Phys. Rev. Lett. **77**, 3276 (1996).

[30] B. D. Esry, C. H. Greene, J. P. Burke, Jr., and J. L. Bohn, Phys. Rev. Lett. **78**, 3594 (1997).

[31] B. D. Esry, Ph.D. dissertation, University of Colorado, 1997 (unpublished).

[32] H. Pu and N. Bigelow, Phys. Rev. Lett. **80**, 1130 (1998).

[33] B.D. Esry and C.H. Greene, Nature (London) **392**, 434 (1998).